Trace element uptake in fresh and aged aluminium oxyhydroxysulfates and hydroxides: Implications for mine drainage-affected environments

Patricia Acero [a], Karen A. Hudson-Edwards [b,*]

[a] *Department of Earth and Planetary Sciences, Birkbeck, University of London, Malet St., London, WC1E 7HX, UK*
[b] *Environment & Sustainability Institute and Camborne School of Mines, University of Exeter, Penryn, TR10 9FE, UK*

ARTICLE INFO

ABSTRACT

Aluminium oxyhydroxysulfates and hydroxides are known to precipitate from mining-generated acidic, neutral and basic pH drainage waters that are enriched in potentially toxic metal(loid)s. Their role as medium-term (1 year) sinks of Al, As, Cu and Ni at pH values of 4, 7 and 10 was assessed using batch experiments. X-ray diffraction analysis showed that basaluminite initially formed at pH 4 and 7, whereas at pH 10, bayerite or nordstrandite (both Al(OH)$_3$) formed. After 12 months of ageing at 20 °C, some of the pH 4 basaluminite recrystallised to form alunite, the pH 7 basaluminite recrystallised to form gibbsite, and the bayerite/nordstrandite was unchanged. At pH 4, the basaluminite took up As but did not take up Ni or Cu. By the end of the 12 months, some As was released from the basaluminite or alunite, and some Cu was taken up by these phases. At the beginning of the pH 7 experiments, As, Cu and Ni were taken up in the basaluminite, and these were retained in the gibbsite that replaced the basaluminite after 12 months. In the pH 10 experiments, only As was expelled from the bayerite/nordstrandite after 12 months. The differences in uptake of As, Cu and Ni are attributed to their aqueous speciation relative to the net surface charge of the Al oxyhydroxsulfates and hydroxides. Release of As from the pH 4 and pH 10 phases at 12 months was likely due to incorporation within the poorly crystalline original phases, followed by progressive release as the phases transformed to more crystalline minerals (at pH 4) or become more crystalline (at pH 10) with ageing. The results have significant implications for the mineralogy of Al oxyhydroxysulfates and hydroxides, and the cycling of As, Cu and Ni, in mine drainage systems.

1. Introduction

Mining activities can generate acidic, neutral and basic pH drainage waters that are enriched in potentially toxic metallic and metalloid elements, such as Al, As, Cu or Ni (Nordstrom, 2011b), that pose hazards to receiving ecosystems (Niyogi et al., 2002). Aluminium oxyhydroxysulfates and hydroxides are known to precipitate from these waters. For example, solid-phase analyses have identified nanoparticulate, poorly crystalline basaluminite (Al$_4$(SO$_4$)(OH)$_{10}$·4H$_2$O) and hydrobasaluminite (Al$_4$(SO$_4$)(OH)$_{10}$·15H$_2$O) as the dominant Al phases formed when acid mine drainage is mixed with circumneutral buffered pH waters (Nordstrom and Alpers, 1999; Bigham and Nordstrom, 2000; Jones et al., 2011; Carrero et al., 2017a). Alunite (KAl$_3$(SO$_4$)$_2$(OH)$_6$) and gibbsite (Al(OH)$_3$) have also been shown to form in acidic mine pit lakes (Kim, 2015; Sánchez-España et al., 2012; 2016). Aluminium oxyhydroxysulfates also form as a result of the dissolution of aluminosilicates or aluminium oxides in the presence of sulfate at pH above 5

(Jambor et al., 2000), and basaluminite has also been identified as one of the main Al minerals precipitating in acid soils (Adams and Rawajfih, 1977; Prietzel and Hirsch 1998). Even though basaluminite and hydrobasaluminite are the main fresh Al precipitates associated with acid waters and soils, it is known that these phases are metastable and tend to gradually transform into more crystalline phases such as alunite (Nordstrom, 1982; Prietzel and Hirsch, 1998) and nanoboehmite (Lozano et al., 2018). This ageing transformation has been successfully reproduced in relatively short periods (around 15 weeks) under controlled laboratory conditions both at 20 °C and 50 °C (Adams and Rawajfih, 1977; Adams and Hajek, 1978; Prietzel and Hirsch, 1998; Prietzel and Mayer, 2005; Singh, 1982).

The oxyhydroxysulfates or hydroxides of Al formed during the neutralization of acidic streams or soil seepage can scavenge dissolved cations and anions depending on their charge (Stumm and Morgan, 2012), which is mainly controlled by the solution pH. Whereas the role as trace element sinks of common Fe-bearing oxyhydroxysulfates such as

jarosite (KFe$_3$(SO$_4$)$_2$(OH)$_6$] and schwertmannite (Fe$_8$O$_8$(OH)$_6$SO$_4$) has already been extensively studied (for a thorough review, see Nordstrom, 2011a), much less is known about the role of Al oxyhydroxysulfates and hydroxides in these processes. Studies to date show that the precipitation of amorphous or microcrystalline Al oxyhydroxysulfates may scavenge trace metals from acid waters (Lee et al., 2002; Munk et al., 2002; Sánchez-España et al., 2006; Carrero et al., 2015). However, their behaviour during the progressive transformation of precipitated phases into more crystalline minerals with ageing remain unknown. Both questions are key to assess the possible role of Al oxyhydroxysulfates and hydroxides as temporary or permanents sinks for trace elements in mine-waste affected and natural environments, and treatment systems for potentially toxic trace metals and metalloids. This study fills this knowledge gap by determining the extent and processes of uptake of As, Cu and Ni by Al oxyhydroxysulfates and hydroxides in acid (pH 4), neutral (pH 7) and alkaline (pH 10) mine drainage-simulated solutions, and how this uptake is affected by ageing of the Al phases over 12 months. The name 'basaluminite' was discredited by the International Mineralogical Association in 2006 (it is a microcrystalline variety of felsöbányaite; Farkas and Pertlik, 1997; Jambor et al., 1998). However, we use it in this manuscript because of its pervasiveness in the scientific literature and in thermodynamic databases (c.f., Sánchez-España et al., 2011; Acero and Hudson-Edwards, 2018). Carrero et al. (2017c) also suggested that the status of basaluminite be re-evaluated to acknowledge its occurrence as a nanomineral.

2. Methods and materials

2.1. Analytical, mineralogical and other techniques

Al oxyhydroxysulfates and hydroxides were synthesised by mixing a 0.02 M solution of Al$_2$(SO$_4$)$_3$ with around 1100 ppb of As(V), Ni(II) and Cu(II) (typical of AMD environments, Nordstrom, 2011b) at an initial pH of 3.35. The concentrations of Al and sulfate were selected to allow precipitation processes to take place and to obtain the required amounts of precipitates for mineralogical determinations. In the case of As, Ni and Cu, their initial concentrations were selected to be high enough to minimise analytical problems (taking into account that large dilution factors are required) but trying to avoid their direct precipitation as pure secondary phases under the pH and sulfate concentrations present in the experiments.

The required amounts of trace elements were obtained by dissolving Na$_2$HAsO$_4$·7H$_2$O (for As), CuSO$_4$ (for Cu) and NiSO$_4$ (for Ni). KOH 1M was then added to this solution dropwise over several minutes to create solutions with pH values of c. 4, 7 and 10 (similar to acidic drainage and to neutralization conditions). All experiments were conducted in duplicate. The solutions were aged at 20 °C, and the pH was monitored every 2–10 days (more frequently at the beginning of the experiments). The pH values of 4, 7 and 10 were maintained by adding either KOH or H$_2$SO$_4$ dropwise while stirring. At the beginning of the experiment the solutions were stirred every day but after one month, they were stirred once every three days. Towards the end of the experiment, stirring was conducted once a week. Watch glasses were placed on top of the beakers to prevent evaporation and maintain a constant solid to solution ratio.

Aqueous samples were taken periodically after the beakers were first stirred while measuring the pH. A 10 mL sample of the solid-solution suspension was then taken and filtered through a 0.2 µm filter. This sample was acidified with HNO$_3$ and stored at 4 °C until analysis. Solid samples were taken after stirring the beaker, and by extracting a 30 mL sample of the suspension and filtering this through a fine mesh Whatman paper. The remaining solid was then washed with 18 MΩ de-ionised water and dried at 20 °C. The dried samples were stored in plastic vials at 20 °C until XRD determinations. The solid: solution ratio was assumed to be constant throughout all of the experiments because only well-mixed suspensions were sampled.

Concentrations of Al, K and S in the terminal slurries involved in this

study were obtained via Inductively Coupled Plasma Optical Emission Spectrometry (ICP-OES) on a Varian 720-ES (axial configuration) using a simultaneous solid-state detector (CCD). Calibration with sets of five standards was performed and laboratory standards were also analysed after every 10 samples and any drift in the measurements (generally less than 4%) was corrected accordingly. The quantification limits for K, Al and S were determined to be 2.6, 3.7 and 3.1 µmol L^{-1}, respectively, and the concentrations of the three elements were determined in the same run. Sulfur concentrations in the sampled solutions are reported as dissolved sulfate because this is the main stable species under the experimental conditions. To aid in determination of the phases that formed in the fresh and aged precipitates, speciation-solubility calculations using the experimental pH and temperature conditions and the measured concentrations of Al, K and S were carried out using the PHREEQC code (Parkhurst and Appelo, 2013) and the wateq4f.dat (Ball and Nordstrom, 1991) thermodynamic database distributed with the code. The dissolution reactions and corresponding log(K) values used to calculate the saturation indices by PHREEQC are shown in Table S1.

Dissolved concentrations of As, Cu and Ni in all the aqueous samples taken over the year of the experiment while the suspensions were stirred were obtained via Inductively Coupled Plasma Mass Spectrometry (ICP-MS) on a Bruker 820-MS-ICP-MS. Calibration with sets of five standards was performed and laboratory standards were also analysed after every 10 samples and any drift in the measurements (generally less than 4%) was corrected accordingly. The quantification limits for As, Cu and Ni 0.5, 1.6 and 0.3 µmol L^{-1}, respectively.

X-ray diffraction (XRD) was carried out using a D/max 2500 RIGAKU diffractometer with a rotating Cu anode at 40 kV and 80 mA. Data were collected using CuKα radiation over the 2θ range from 2.5° to 80°, with step = 0.03 and a collection time of 2s/step. Mineral identification was carried out by comparison of the resultant peaks on the XRD spectra with those in the Powder Diffraction File (PDF) database provided by the International Centre for Diffraction Data (ICDD).

3. Results and discussion

3.1. Formation of Al oxyhydroxysulfates and hydroxides, and changes in mineralogy with time

The major element concentrations for the pH 4, 7 and 10 experiments are shown in Tables S2, S4 and S6, respectively, and the calculated
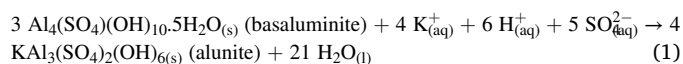
Table 1

XRD and PHREEQC modelling results. Al(OH)$_3$(a) = amorphous aluminium hydroxide.

XRD Analysis	pH 4	pH 7	pH 10
Initial	Basaluminite	Basaluminite	Bayerite, Nordstrandite
Aged 12 months	Basaluminite + Alunite	Gibbsite	Bayerite, Nordstrandite
PHREEQC Analysis	**Equilibrium (SI ≈ 0)**	**Oversaturated (SI > 0)**	
pH ≤ 5	Gibbsite	Basaluminite, Alunite, Diaspore	
pH 5.5–6	Al(OH)$_3$(a)	Basaluminite, Alunite, Diaspore, Gibbsite	
pH 6.5–8	–	Basaluminite, Alunite, Diaspore, Gibbsite, Al(OH)$_3$(a)	
pH 10	–	Diaspore, Gibbsite	
Mineral	**Formula**		
Alunite	KAl$_3$(SO$_4$)$_2$(OH)$_6$		
Basaluminite	Al$_4$(SO$_4$)(OH)$_{10}$·4H$_2$O		
Diaspore	AlOOH		
Gibbsite, Bayerite, Nordstrandite	Al(OH)$_3$		

saturated indices for the phases shown in Table 1 are compiled in Tables S3, S5 and S7, respectively. Speciation-solubility calculations using PHREEQC and the wateq4f.dat database for the compositions of the terminal slurries show that the solutions of pH 4 and 7 are close to equilibrium or oversaturated with respect to basaluminite, alunite, gibbsite and diaspore (AlOOH) (Table 1). In the case of the solutions under pH 7, they seem to be also oversaturated with respect to amorphous aluminium hydroxide ($Al(OH)_3(a)$). In contrast to these results, the solutions at pH 10 are predicted to be oversaturated only with respect to gibbsite and diaspore (Table 1). We are confident of the identification of all of these phases except $Al(OH)_3(a)$, because they produce clear XRD peaks that facilitate their identification (Fig. 1). We appreciate that, because $Al(OH)_3(a)$ may not be identified by XRD due to its poor crystallinity, our suggestion of its presence is hypothetical.
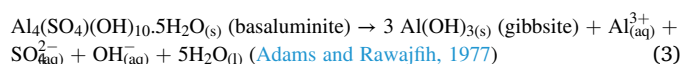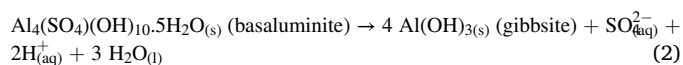
XRD results agree, in general, with the PHREEQC calculations. The XRD spectrum for the initial pH 4 solid matches that of basaluminite, and that for the aged pH 4 solid seem to correspond to a mixture of basaluminite and alunite (Fig. 1). A possible overall reaction to describe such evolution of basaluminite in the presence of K^+, H^+ and SO_4^{2-}, to form alunite could be:

$$3 \ Al_4(SO_4)(OH)_{10}.5H_2O_{(s)} \text{ (basaluminite)} + 4 \ K^+_{(aq)} + 6 \ H^+_{(aq)} + 5 \ SO_4^{2-}_{(aq)} \rightarrow 4 \ KAl_3(SO_4)_2(OH)_{6(s)} \text{ (alunite)} + 21 \ H_2O_{(l)} \quad (1)$$

In both basaluminite and alunite, the Al atoms are bonded with 6 oxygen to form Al octahedra, and these octahedra are organised in layers with interstitial SO_4^{2-} ions (Hawthorne et al., 2000). In reaction (1) the octrahedra are likely re-organised, and K^+ introduced in the 12-fold co-ordinated interstitial vacancies, to form alunite. The conversion of basaluminite to alunite has been observed previously, and it is kinetically inhibited, occurring very slowly and sometimes incompletely (Adams and Rawajfih, 1977; Nordstrom, 1982; Prietzel and Hirsch, 1998; Prietzel and Mayer, 2005). The conversion has been proposed to be a re-dissolution/re-precipitation process in solutions with K^+ activities greater than 10^{-5} mol^{-1} (Adams and Rawajfih, 1977; Nordstrom, 1982), as basaluminite has been shown to dissolve readily at pH < 4 (Acero and Hudson-Edwards, 2018).

The XRD spectra for the initial pH 7 precipitates match those of basaluminite, and those for the aged precipitate point towards the presence of gibbsite (Fig. 1, Table 1). The formation of gibbsite from basaluminite could be described according to one of the following incongruent reactions, the first being acid-generating and the second base-generating:

$$Al_4(SO_4)(OH)_{10}.5H_2O_{(s)} \text{ (basaluminite)} \rightarrow 4 \ Al(OH)_{3(s)} \text{ (gibbsite)} + SO_4^{2-}_{(aq)} + 2H^+_{(aq)} + 3 \ H_2O_{(l)} \quad (2)$$

$$Al_4(SO_4)(OH)_{10}.5H_2O_{(s)} \text{ (basaluminite)} \rightarrow 3 \ Al(OH)_{3(s)} \text{ (gibbsite)} + Al^{3+}_{(aq)} + SO_4^{2-}_{(aq)} + OH^-_{(aq)} + 5H_2O_{(l)} \text{ (Adams and Rawajfih, 1977)} \quad (3)$$

For the experiments at pH 7 carried out in this study, it was necessary to periodically correct pH drifting towards lower pH values by means of KOH addition. In the light of such trends, an overall reaction similar to (2) (acid-generating basaluminite-gibbsite conversion) seems to be favoured throughout the experiments. During this reaction, the basaluminite structure breaks down, likely releasing sulfate ions, water molecules and protons and the Al octahedral sheets are hydrogen-bonded to form gibbsite.

The XRD spectra for the pH 10 initial and aged precipitates match those of bayerite and nordstrandite (both $Al(OH)_3$) (Fig. 1, Table 1). Basaluminite is not known to form under pH conditions above 7.5 (Bigham and Nordstrom, 2000). The stable Al phase reported in earlier studies for those solutions seems to be $Al(OH)_3$ (Bigham and Nordstrom, 2000; Sánchez-España et al., 2012; 2016), in agreement with our results. The observed mineralogical evolution in the present study is also consistent with the earlier work by Schoen and Roberson (1970), who proposed that gibbsite ages to form bayerite, which later transforms into nordstrandite.

Our XRD and PHREEQC speciation calculations presented in Table 1 largely agree with those for other experimental and natural mine waste and other systems. Aluminum has been shown to hydrolyse and be removed from solution by precipitation above pH 4.5 (Nordstrom and Ball, 1986; Lükewille and van Breemen, 1992; Bigham and Nordstrom, 2000) as the major dissolved species of Al change from Al^{3+} to $Al(OH)^{2+}$ (Martell and Motekaitis, 1989; Bigham and Nordstrom, 2000). Bigham and Nordstrom (2000) suggested that amorphous $Al(OH)_3$ or basaluminite formed from solutions with pH values between 4 and 7.5. Similar observations have also been reported in more recent studies focused on acid sulfate soils (Jones et al., 2011) and even near the bottom of acidic pit lakes (Sánchez-España et al., 2011). Lozano et al. (2018) showed that basaluminite dissolved incongruently between pH 4.95 and near-neutral values, forming amorphous Al-hydroxide, which in turn recrystallised to form nanoboemite over 81 days.

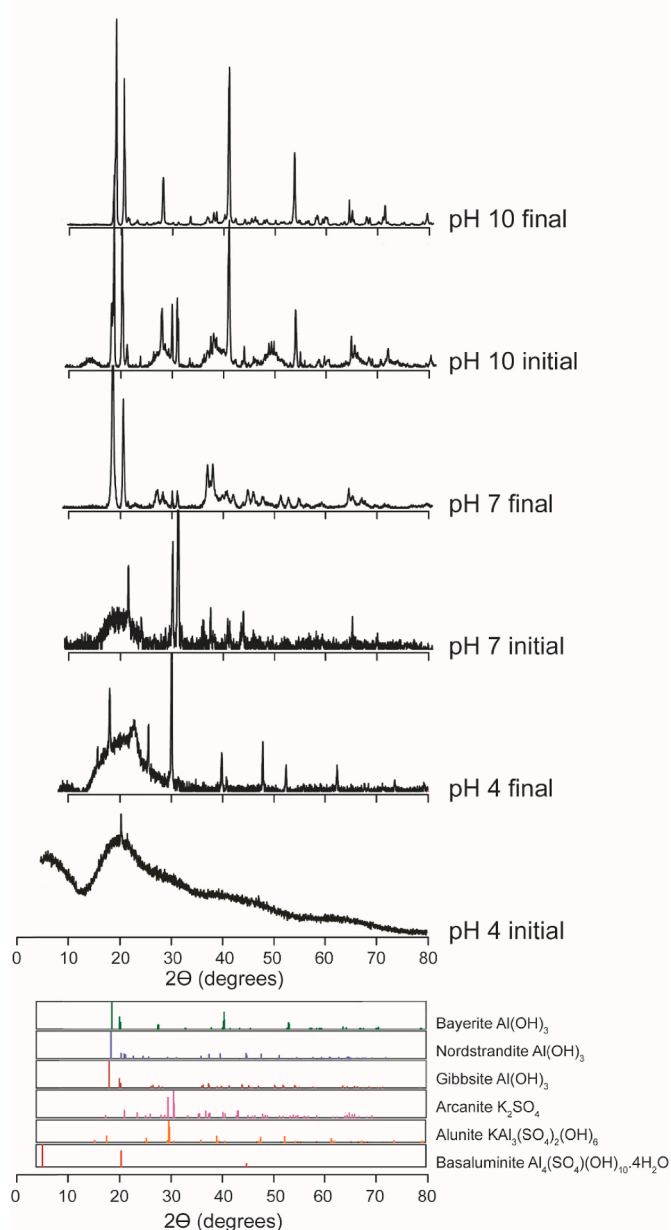Poorly crystalline and metastable basaluminite and amorphous Al

Fig. 1. XRD patterns for initial and 12-month aged Al oxyhydroxysulfates and hydroxides at pH 4, 7 and 10.

(OH)$_3$ have been reported to transform with time into more crystalline alunite and gibbsite (Nordstrom, 1982; Prietzel and Hirsch, 1998). In pit lakes in Rio Tinto area, Sánchez-España et al., 2012, 2016) reported stable alunite up to pH 4, basaluminite forming between pH 4 and 6 and gibbsite precipitating under pH values above pH 6. Adams and Hajek (1978) and Singh (1982) have shown that mixtures of gibbsite, basaluminite and alunite are generated by the ageing of acidic aluminum sulfate solutions. Our XRD spectra shown in Fig. 1 indicate that the crystallinity of the samples (as shown by the change from broad diffuse peaks to sharp peaks) strongly increases with aging and with increasing pH.

3.2. Evolution of trace element concentrations in the supernatants during the experiments

In this section, the evolution of the concentrations measured in the supernatant solutions for the target trace elements (As, Cu and Ni) will be described. The trace element concentrations for the pH 4, 7 and 10 experiments are reported in Tables S8, S10 and S12, respectively. Saturation indices for selected Ni and Cu phases for the pH 4, 7 and 10 experiments are reported in Tables S9, S11 and S13, respectively.

3.2.1. Experiments at pH 4
For the experiments at pH c. 4, the concentrations of Cu and Ni after one day of the formation of precipitates were very similar to the original concentrations (around 1100 µg L^{-1}) in the initial solutions before the

Fig. 2. Evolution of dissolved concentrations in the supernatants for **(a)** the trace elements included in this study (As, Cu and Ni) during the experiment at pH c. 4 and **(b)** for the concentrations of As during the experiments at pH c. 10. For the rest of the elements and for the experiments at pH c. 7, all dissolved concentrations in the supernatants were below the quantification limit during the experiments.

pH adjustment and formation of precipitates (Fig. 2a). The dissolved concentrations of Ni remained around the initial values throughout the entire experiment, and the concentrations of Cu in the supernatant only remained around these values for the former six months of experiments, decreasing thereafter to values below the quantification limit at the end of the experiments (Fig. 2a).

In contrast to this behaviour, As concentrations in the same solutions decreased after some days of precipitate formation to less than 500 µg L^{-1} and then decreased even more in the samples after one month of experiment to values generally below 300 µg L^{-1} (but above the quantification limit) for the rest of the experiment (Fig. 2a).

3.2.2. Experiments at pH 7 and 10
The concentrations of all the studied trace elements in the experiments at pH 7 and 10 decreased in the first sampled solution after precipitate formation to concentrations below the quantification limit (not shown). For Cu and Ni, the dissolved concentrations in the sampled supernatants remained similarly low throughout the entire experiments both at pH c. 7 and c. 10 (not shown). A similar evolution was observed for As concentrations in the experiments at pH c. 7.

In contrast, the dissolved As concentrations in the experiments at pH c. 10 increased steadily in the subsequent supernatant solutions, reaching values above 400 µg L^{-1} in the last supernatants after one year of precipitate-solution interaction (Fig. 2b). This increase in As concentrations was particularly rapid during the first six months of experiment.

3.3. Possible processes involved in the observed evolution of the concentrations of trace elements in the supernatants

The variations for the different elements and experimental pH in the solutions, described in the previous section, are likely attributable to: (1) changes in the type of precipitated phases and in the surface charge of the mineral sorbants with solution pH, and (2) differences in the speciation of each trace element under different pH conditions. These possible influences and processes will be described here with the assistance of speciation-solubility calculations and taking into account the mineralogical results above.

According to the XRD results, the precipitated phases for all the studied conditions include different types of aluminium hydroxides (gibbsite, bayerite and nordstrandite) and oxyhydroxysulfates (basaluminite). For the interpretation of interactions between the surfaces of these precipitates and the target dissolved trace elements under various pH conditions, one of the critical parameters is the point of zero charge (PZC). The PZC is the pH value at which the surface of the adsorbant is globally neutral (i.e. equal number of positive and negative charges) (e. g. Birdi, 2015). The adsorbant surface has a net positive charge for pH values below the PZC and a net negative charge for pH values above the PZC.

The PZC has been reported to be above pH 8 for different aluminum hydroxides including gibbsite and amorphous Al(OH)$_3$ (see compilation by Kosmulski, 2016), and at pH 9.5–10 for pristine gibbsite specifically (Huang et al., 2002). Although the PZC for basaluminite has not been reported yet (to the best of our knowledge), it could be assumed to be net positive charge under pH conditions of both 4 and 7, which would favor the uptake of anionic species by surface-solution interactions. On the other hand, the surface of the observed precipitates (bayerite/nordstrandite) in the experiments at pH 10 would have a net negative charged surface, favoring the uptake of cationic species.

The preferential uptake of As at pH 4 (Fig. 2) may be due to its occurrence mainly as H$_2$AsO$_4^-$ (Fig. 3), which would be attracted to the net positive charge of the surface of both basaluminite and alunite. In contrast, the lack of sorption of Cu and Ni (Fig. 2) can be attributed to their predominant occurrence as neutral (CuSO$_4$ and NiSO$_4$) or cationic dissolved species (Cu^{2+} and Ni^{2+}) (Fig. 3). The coprecipitation of these elements into basaluminite does not seem to be favoured either under
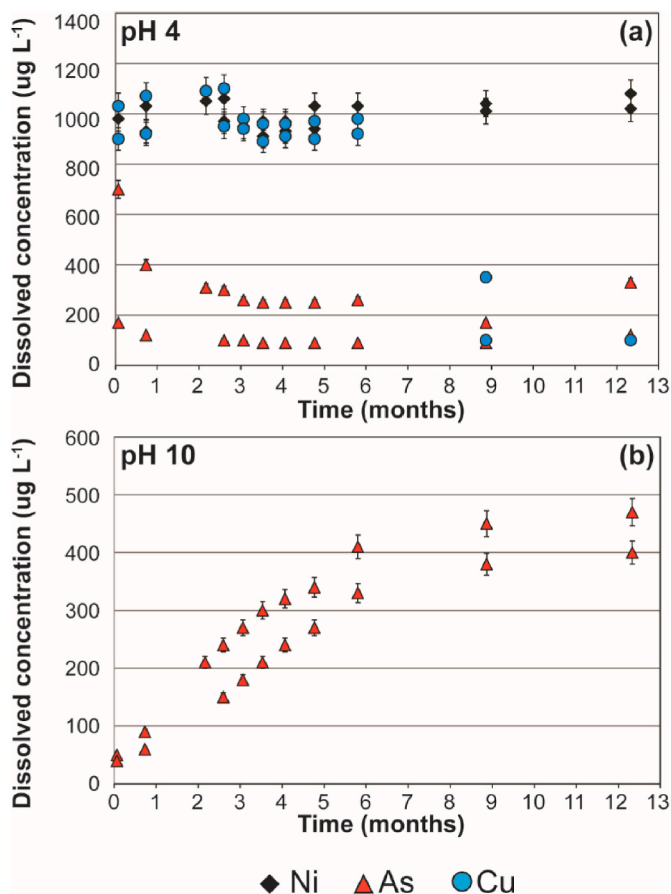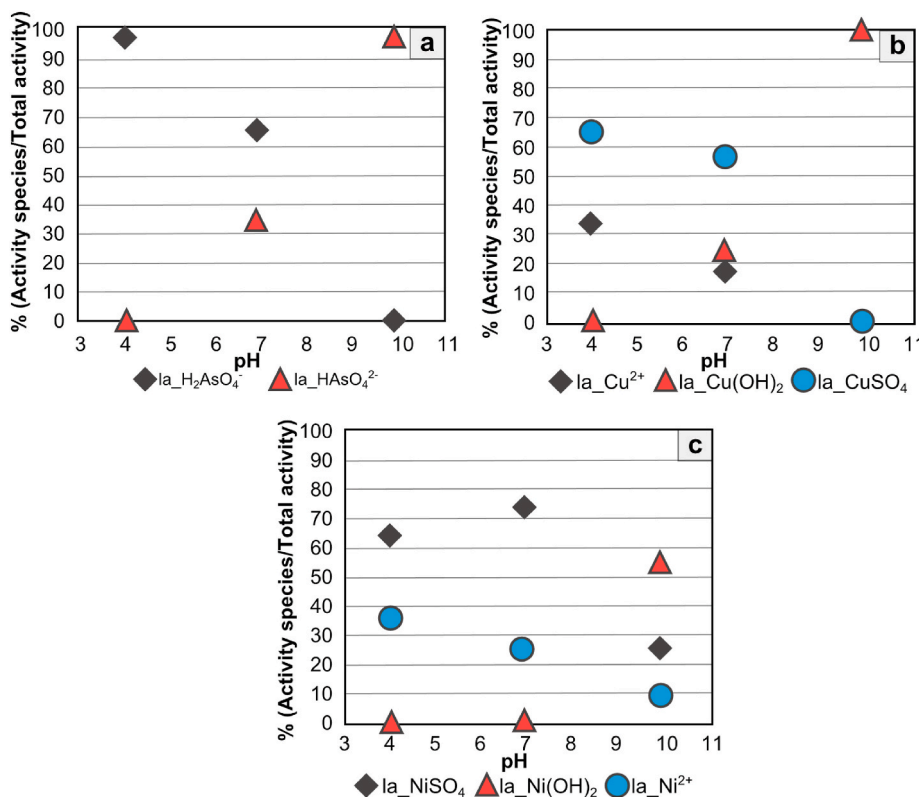
Fig. 3. Speciation of dissolved **(a)** As, **(b)** Cu and **(c)** Ni, expressed as the percentage with respect to total activity calculated by PHREEQC for the experiments under the three target pH conditions studied in this work (c. pH 4, 7 and 10). Only the species representing more than 10% of the activity for each studied trace element are displayed in the plots.

these conditions.

For Cu, the decrease of dissolved concentrations observed in the supernatant samples after 6 months (Fig. 2) does not seem to be related to any change in the speciation of this element or in the mineral sorbant-solution interaction. According to the solubility calculations, the precipitation of the Cu mineral phases included in the thermodynamic database is not favoured either (Tables S9, S11, S13). A possible explanation for the observed evolution of Cu concentrations in the last part of the experiments at pH c. 4 would be incorporation of Cu by substitution for Al^{3+} coupled with the creation of an OH^- vacancy (cf., Hudson-Edwards and Wright, 2011) in alunite, which is forming by aging during this stage. Unfortunately, this hypothesis cannot be discussed further with the currently available information, but further research on this topic is granted.

In the case of the experiments at pH 7, the dissolved concentrations of all the target elements decreased rapidly after basaluminite formation to values below the quantification limit, remaining similarly low for the rest of the experiment (not shown). Although not detectable by XRD, the precipitation of amorphous $Al(OH)_3$ under these experimental conditions is also possible according to solubility calculations (Tables 1 and S5), which should be taken into account in order to explain the observed evolution.

As explained above, if the PZC for basaluminite is assumed to be above pH 8 (similar to other aluminum hydroxides including amorphous $Al(OH)_3$; Kosmulski, 2016), the net surface charge of the mineral sorbants would be positive at pH 7. Since the main dissolved As species for these experiments are calculated to be the anionic species $H_2AsO_4^-$ and $HAsO_4^{2-}$ (Fig. 3a), this surface charge could explain the observed decrease of As concentrations (by sorption). For Cu and Ni, their main calculated dissolved species are $CuSO_4$, $Cu(OH)_2$ and Cu^{2+} (for Cu; Fig. 3b) and $NiSO_4$ and Ni^{2+} (for Ni; Fig. 3c). The uptake of the cationic species of both trace elements (Cu^{2+} and Ni^{2+}) by surface-solution

interactions would not be favoured at pH 7.

In the light of solubility calculations, the precipitation of either Cu or Ni mineral phases is not favoured under these pH conditions. Another possibility would be the incorporation of both elements to the structure of precipitating basaluminite or amorphous $Al(OH)_3$, by coprecipitation or in the form of surface precipitates (due to a local supersaturation at the mineral-water interface, as explained for instance in Sparks, 2003). For example, Chang et al. (2005) showed, using EXAFS, that neutral Cu $(OH)_2^0$ species eventually formed surface $Cu(OH)_2$ precipitates on the surface of gibbsite above pH 5.63. Scheckel and Sparks (2000) demonstrated that $Ni(OH)_2$ precipitates formed on gibbsite-silica surfaces at pH 7.5, and over a year, these aged to form a Ni phyllosilicate. Although our calculated saturation indices for $Ni(OH)_2$ and $Cu(OH)2$ are negative for the pH 7 experiments (−3.37 to −4.00 and −1.52 to −2.11, respectively; Table S11), they are weakly so, and thus precipitation of these phases may have been possible. More structural information, not available at this point of research, would be key to fully understand the relative importance of these processes. In any case, the aging of precipitates and the associated transformation of initial basaluminite (and possibly amorphous $Al(OH)_3$) into more crystalline gibbsite does not seem to be associated with any release of As, Cu and Ni, whose dissolved concentrations remained below their quantification limits throughout this process until the end of the experiments at pH 7.

Our results in the experiments at pH c. 4 and 7 are in agreement with earlier studies. Lee et al. (2002) found that more than 90% of the Cu and Ni were removed by aluminum amorphous precipitates ($AlOHSO_4$ and basaluminite) between pH 4 and 6. During neutralization experiments involving AMD from the Snake River, Colorado, white Al precipitates that were proposed to be Al oxyhydroxysulfates and $Al(OH)_3$ were shown to sorb divalent metal cations (Munk et al., 2002). At pH 4.8, 75% of the original Cu was sorbed, and only 18% of the Ni was sorbed. In the same study, Cu and Ni were reported to be completely sorbed at pH

values of 6.4 and 6.7, respectively. Simón et al. (2005) demonstrated that Al oxyhydroxysulfates were involved in removing As and Cu (among other elements) from pH 3.5–6.5 solutions generated by the oxidation of pyrite tailings and reaction with limestone particles. Consistent results have recently been proposed by Robertson et al. (2016), who showed that Al oxyhydroxysulfates (proposed to contain some basaluminite) from uranium mill raffinate were able to uptake almost all of the As (between 2.78 and 341 mg/L) from pH 4 solutions. Sánchez-España and Reyes (2019) have also demonstrated that hydrobasaluminite formed from neutralization of metal-rich mine waters takes up significant amounts of Cu (3.7–7.1 wt) and Ni (209–1821 ppm). Wanner et al. (2018) showed that As-bearing basaluminite also precipitated from an acidic (pH ~ 4) stream in Switzerland, and Carrero et al. (2017b) showed that synthetic basaluminite was effective in taking up As(V).

For the experiments at pH 10, the net surface charge of precipitates (bayerite and nordstrandite) can reasonably assumed to be negative throughout the experiments. For dissolved As, the only relevant species according to speciation calculations is $HAsO_4^{2-}$ (Fig. 3a), which theoretically should not be attracted to the negatively charged precipitate surfaces. Since As dissolved concentrations are observed to decrease at the beginning of the experiments to values close to the quantification limit of 40 μg L^{-1} (Fig. 2b), other processes different from surface-solution interactions seem to be responsible for the As uptake by aluminum precipitates. Solubility calculations do not cast much light on this observed behaviour due to the scarcity of thermodynamic data on As phases that could be of interest. Apart from the possible direct precipitation of small amounts of such hypothetical phases, the main other possibility to account for the observed As trends in the experiments at pH c.10 would be the incorporation of As to the lattice of the forming aluminum hydroxides and then its progressive release with aging as they become structurally more ordered. This would explain the observed initial decrease in As dissolved concentrations and then its release during the rest of the experiment (Fig. 2b). This is confirmed by the work of Masue et al. (2007), who observed low amounts of As(V) adsorption to 1:1 and 1:0 Al:Fe hydroxides, and attributed this to low numbers of surface sorption sites on bayerite and gibbsite due to Al^{3+} being fully coordinated to OH^- groups on the surface and therefore unavailable for bonding. According to this, the ageing of the likely less crystalline initial $Al(OH)_3$ to more crystalline bayerite or nordstrandite in our experiments would result in lower availability of surface Al^{3+} for bonding with the $HAsO_4^{2-}$, and release of the As (Fig. 2b).

In the case of Ni, the simplest explanation would be the precipitation of this element as $Ni(OH)_2$, which seems to be thermodynamically favoured according to solubility calculations (Table S13). Apart from this and according to speciation calculations, most of the dissolved Ni is present as neutral species ($Ni(OH)_2$ and $NiSO_4$), with around a 10% present as the cationic species Ni^{2+} (Fig. 3c). The uptake of all these species could also account for the observed decrease of Ni concentrations to values below the quantification limit throughout the entire experiments at pH c.10.

Finally, Cu concentrations were below the quantification limit during the whole of the experimental runs. This behaviour could be due to both the uptake of the neutral $Cu(OH)_2$ species (the only relevant one at this pH; Fig. 3b) by surface processes or to the coprecipitation of Cu with the forming aluminum hydroxides. In contrast to Ni, solubility calculation results for Cu do not support the direct precipitation of any mineral of this element included in the thermodynamic database, although the saturation indices for $Cu(OH)_2$ have low negative values (Table S13).

4. Conclusions

The aim of this study was to determine to what extent As, Cu and Ni were taken up by Al oxyhydroxysulfates and hydroxides in acidic to alkaline mine drainage analogue solutions, and how ageing over 12 months affected the mineralogy of the Al phases and the retention of

their incorporated trace elements. At pH 4, only As was taken up by the initially-formed basaluminite, and this was mostly retained by the basaluminite and alunite that remained at the end of the 12 months. At pH 7, As, Cu and Ni were all taken up by the initially-formed basaluminite, and all were retained over the 12 months as the mineral recrystallised to gibbsite. At pH 10, all three trace elements were taken up initially by the bayerite/nordstrandite. Copper and Ni were retained in the solid phase as the minerals recrystallised, but As was progressively released to solution over the 12 months of ageing.

The mineralogical transformation results agree with previous studies on the evolution of Al oxyhydroxysulfates and hydroxides, but provide new insights into the timescales of changes and on the impact of incorporated trace elements on these changes. The study has demonstrated significant differences in As, Cu and Ni behaviour with pH and mineralogy, which are in turn attributed to trace element speciation and mineral surface charge. To better understand the impact of mining on the environment, further work is required to understand the behaviour of these and other common mine waste contaminants (e.g., Pb, Sb, Zn) in Al-, S- and O-bearing natural and synthetic systems.

Declaration of competing interest

The authors declare the following financial interests/personal relationships which may be considered as potential competing interests: Patricia Acero reports that finance was provided by European Commission Marie Curie Intra-European Fellowship.

Data availability

Data will be made available on request.

Appendix A. Supplementary data

Supplementary data to this article can be found online at https://doi.org/10.1016/j.apgeochem.2022.105444.

References

Adams, F., Hajek, B.F., 1978. Effects of solution sulfate, hydroxide and potassium concentrations on the crystallisation of alunite, basaluminite and gibbsite from dilute aluminium solutions. Soil Sci. 126, 169–173.

Adams, F., Rawajfih, Z., 1977. Basaluminite and alunite: a possible cause of sulfate retention by acid soils. Soil Sci. Soc. Am. J. 41 (4), 686–692.

Acero, P., Hudson-Edwards, K.A., 2018. Influence of pH and temperature on basaluminite dissolution rates. ACS Earth Space Chem 2, 203–209.

Ball, J.W., Nordstrom, D.K., 1991. User's manual for WATEQ4F, with revised thermodynamic database and test cases for calculating speciation of major, trace, and redox elements in natural waters. U.S. Geol. Surv. Open-File Rep. 91–183, 189.

Bigham, J.M., Nordstrom, D.K., 2000. Iron and aluminium hydroxysulfates from acid sulfate waters. In: Alpers, C.N., Jambor, J.L., Nordstrom, D.K. (Eds.), Sulfate Minerals - Crystallography, Geochemistry, and Environmental Significance. Mineral. Soc. Amer. 40, Washington, DC, pp. 351–403.

Birdi, K.A.S. (Ed.), 2015. Handbook of Surface and Colloid Chemistry. CRC Press.

Carrero, S., Pérez-López, R., Fernandez-Martinez, A., Cruz-Hernández, P., Ayora, C., Poulain, A., 2015. The potential role of aluminium hydroxysulphates in the removal of contaminants in acid mine drainage. Chem. Geol. 417, 414–423.

Carrero, S., Fernandez-Martinez, A., Pérez-López, R., Nieto, J.M., 2017a. Basaluminite structure and its environmental implications. Proc. Earth Planet. Sci 17, 237–240.

Carrero, S., Fernandez-Martinez, A., Pérez-López, R., Poulain, A., Salas-Colera, E., Nieto, J.M., 2017b. Arsenate and selenite scavenging by basaluminite: insights into

the reactivity of aluminum phases in acid mine drainage. Environ. Sci. Technol. 51, 28–37.

Carrero, S., Fernandez-Martinez, A., Pérez-López, Lee, D., Aquilante, G., Poulain, A., Lozano, A., Nieto, J.M., 2017c. The nanocrystalline structure of basaluminite, an aluminum hydroxide sulfate from acid mine drainage. Am. Mineral. 102, 2381–2389.

Chang, T.W., Wang, M.K., Jang, L.Y., 2005. An extended X-ray absorption spectroscopy study of copper(II) sorption by oxides. Geoderma 129, 211–218.

Farkas, L., Pertlik, F., 1997. Crystal structure determinations of felsöbányaite and basaluminite, $Al_4(SO_4)(OH)_{10} \cdot 4H_2O$. Acta Mineral. Petrog. Szeged. 38, 5–15.

Hawthorne, F.C., Krivovichev, S.V., Burns, P.C., 2000. The crystal chemistry of sulfate minerals. In: Alpers, C.N., Jambor, J.L., Nordstrom, D.K. (Eds.), Sulfate Minerals: Crystallography, Geochemistry, and Environmental Significance. Rev. Mineral. Geochem, 40, pp. 1–112.

Hudson-Edwards, K.A., Wright, K., 2011. Computer simulations of the interactions of the (012) and (001) surfaces of jarosite with Al, Cd, Cu2+ and Zn. Geochem. Cosmochim. Acta 75, 52–62.

Huang, P.M., Wang, M.K., Kapmpf, N., Schulze, D.G., 2002. Aluminum hydroxides. In: Dixon, J.B., Schulze, D.G. (Eds.), Soil Mineralogy with Environmental Applications. Soil Sci. Soc. Am., Inc., Madison, WI, pp. 261–289.

Jambor, J.L., Grew, E.S., Roberts, A.C., 1998. New mineral names. Am. Mineral. 83, 1347–1352.

Jambor, J.L., Nordstrom, D.K., Alpers, C.N., 2000. Metal-sulfate salts from sulfide mineral oxidation. In: Alpers, C.N., Jambor, J.L., Nordstrom, D.K. (Eds.), Sulfate Minerals: Crystallography, Geochemistry, and Environmental Significance. Rev. Mineral. Geochem 40, 303–350.

Jones, A.M., Collins, R.N., Waite, T.D., 2011. Mineral species control of aluminium solubility in sulfate-rich acidic waters. Geochem. Cosmochim. Acta 75, 965–977.

Kim, Y., 2015. Mineral phases and mobility of trace metals in white aluminium precipitates found in acid mine drainage. Chemosphere 119, 803–811.

Kosmulski, M., 2016. Isoelectric points and points of zero charge of metal (hydr)oxides: 50 years after Parks' review. Adv. Colloid Interface Sci. 238, 1–61.

Lee, G., Bigham, J.M., Faure, G., 2002. Removal of trace metals by coprecipitation with Fe, Al and Mn from natural waters contaminated with acid mine drainage in the Ducktown Mining District, Tennessee. Appl. Geochem. 17, 569–581.

Lozano, A., Fernández-Martínez, A., Ayora, C., Poulain, A., 2018. Local structure and ageing of basaluminite at different pH values and sulphate concentrations. Chem. Geol. 496, 25–33.

Lükewille, A., van Breemen, N., 1992. Aluminium precipitates from groundwater of an aquifer affected by acid atmospheric deposition in the Senne, Northern Germany. Water Air Soil Pollut. 63, 411–416.

Martell, A.E., Motekaitis, R.J., 1989. Coordination chemistry and speciation of Al(III) in aqueous solution. In: Lewis, T.E. (Ed.), Environmental Chemistry and Toxicology of Aluminum. Lewis Publishers, Boca Raton, FL, USA, pp. 4–17.

Masue, Y., Loeppert, R.H., Kramer, T.A., 2007. Arsenate and arsenite adsorption and desorption behavior on coprecipitated aluminum:iron hydroxides. Environ. Sci. Technol. 41, 837–842.

Munk, L., Faure, G., Pride, D.E., Bigham, J.M., 2002. Sorption of trace metals to an aluminum precipitate in a stream receiving acid rock-drainage; Snake River, Summit County, Colorado. Appl. Geochem. 17 (4), 421–430.

Niyogi, D.K., Lewis, W.M., McKnight, D.M., 2002. Effects of stress from mine drainage on diversity, biomass, and function of primary producers in Mountain Streams. Ecosystems 5, 554–567.

Nordstrom, D.K., 1982. The effect of sulfate on aluminium concentrations in natural waters: some stability relations in the system Al_2O_3-SO_3-H_2O at 298 K. Geochem. Cosmochim. Acta 46 (4), 681–692.

Nordstrom, D.K., 2011a. Hydrogeochemical processes governing the origin, transport and fate of major and trace elements from mine wastes and mineralized rock to surface waters. Appl. Geochem. 26, 1777–1791.

Nordstrom, D.K., 2011b. Mine waters: acidic to circumneutral. Elements 7, 393–398.

Nordstrom, D.K., Alpers, C.N., 1999. Geochemistry of acid mine wastes. In: Plumlee, G. S., Logsdon, M.J. (Eds.), The Environmental Geochemistry of Mineral Deposits, 6A. Society of Economic Geologists, Littleton, CO, pp. 133–160.

Nordstrom, D.K., Ball, J.W., 1986. The geochemical behavior of aluminum in acidified surface waters. Science 232, 54–56.

Parkhurst, D.L., Appelo, C.A.J., 2013. Description of input and examples for PHREEQC version 3: a computer program for speciation, batch-reaction, one-dimensional transport, and inverse geochemical calculations. US Geol. Sur. Techn. Meth. 497 book 6, chap. A43.

Prietzel, J., Hirsch, C., 1998. Extractability and dissolution kinetics of pure and soil-added synthesized aluminium hydroxyl sulphate minerals. Eur. J. Soil Sci. 49 (4), 669–681.

Prietzel, J., Mayer, B., 2005. Isotopic fractionation of sulfur during formation of basaluminite, alunite, and natroalunite. Chem. Geol. 215 (1), 525–535.

Robertson, J., Hendry, M.J., Essilfie-Dugham, J., Chen, J., 2016. Precipitation of aluminium and magnesium secondary minerals from uranium mill raffinate (pH 1.0-10.5) and their controls on aqueous contaminants. Appl. Geochem. 64, 30–42.

Sánchez-España, J., Reyes, J., 2019. Comparing schwertmannite and hydrobasaluminite dissolution in ammonium oxalate (pH 3.0): implications for metal speciation studies by sequential extraction. Minerals 9, 57.

Sánchez-España, J., Yusta, I., Diez, M., 2011. Schwertmannite and hydrobasaluminite: a re-evaluation of their solubility and control on the iron and aluminium concentration in acidic pit lakes. Appl. Geochem. 26, 1752–1774.

Sánchez-España, J., Yusta, I., López, G., 2012. Schwertmannite to jarosite conversion in the water column of an acidic mine pit lake. Miner. Mag. 76–7, 1233–1256.

Sánchez-España, J., López Mao, E., Santofimia Pastor, E., Reyes Andrés, J., Martín Rubí, J.A., 2006. The removal of dissolved metals by hydroxysulphate precipitates during oxidation and neutralisation of acid mine waters, Iberian Pyrite Belt. Aquat. Geochem. 12, 269–298.

Sánchez-España, J., Yusta, I., Gray, J., Burgos, W.D., 2016. Geochemistry of dissolved aluminium at low pH: extent and significance of Al-Fe(III) coprecipitation below pH 4.0. Geochem. Cosmochim. Acta 175, 128–149.

Scheckel, K.G., Sparks, D.L., 2000. Kinetics of the formation and dissolution of Ni precipitates in a gibbsite/amorphous silica mixture. J. Colloid Interface Sci. 229, 222–229.

Schoen, R., Roberson, C.E., 1970. Structures of aluminum hydroxide and geochemical implications. Am. Mineral. 55, 43–77.

Simón, M., Martín, F., García, I., Bouza, P., Dorronsoro, C., Aguilar, J., 2005. Interaction of limestone grains and acidic solutions from oxidation of pyrite tailings. Environ. Pollut. 135, 65–72.

Singh, S.S., 1982. The formation and coexistence of gibbsite, boehmite, alumina and alunite at room temperature. Can. J. Soil Sci. 62, 327–332.

Sparks, D.L., 2003. Environmental Soil Chemistry. Academic Press.

Stumm, W., Morgan, J.J., 2012. Aquatic Chemistry: Chemical Equilibria and Rates in Natural Waters, third ed. John Wiley and Sons, New York.

Wanner, C., Pöthig, R., Carrero, S., Fernande-Martinez, A., Jäger, C., Furrer, G., 2018. Natural occurrence of nanocrystalline Al-hydroxysulfates: insights on formation, Al solubility control and as retention. Geochem. Cosmochim. Acta 238, 252–269.